Inorg. Chem. **2005**, *44*, 5030–5041

Oxygen-Bridged Borate Anions from Tris(pentafluorophenyl)borane: Synthesis, NMR Characterization, and Reactivity

Alessia Di Saverio,[†] Francesca Focante,[†] Isabella Camurati,[†] Luigi Resconi,*[,†] Tiziana Beringhelli,[‡] Giuseppe D'Alfonso,*[,‡] Daniela Donghi,[‡] Daniela Maggioni,[‡] Pierluigi Mercandelli,*[,§] and Angelo Sironi[§]

Basell Polyolefins Italia, P. le Donegani 12, 44100 Ferrara, and Dipartimento di Chimica Inorganica, Metallorganica e Analitica, Facoltà di Farmacia, and Dipartimento di Chimica Strutturale e Stereochimica Inorganica, Università degli Studi di Milano, Via Venezian 21, 20133 Milano, Italy

Received February 9, 2005

The previously known anion $[(C_6F_5)_3B(\mu\text{-}OH)B(C_6F_5)_3]^-$ (**2**) has been prepared by a two-step procedure, involving deprotonation of $(C_6F_5)_3BOH_2$ to give $[B(C_6F_5)_3OH]^-$ (**1**), followed by addition of $B(C_6F_5)_3$. The solution structure and the dynamics of **2** have been investigated by ^1H and ^{19}F NMR spectroscopy. The reaction of $[NHEt_3]$**2** with NEt_3 resulted in the formation of $[NHEt_3]^+[(C_6F_5)_3BOH]^-$, $[NHEt_3]^+[(C_6F_5)_3BH]^-$, and $(C_6F_5)_3B^-(CH_2CH{=}N^+Et_2)$. This indicates that in the presence of a nucleophile anion **2** can dissociate to $B(C_6F_5)_3$ and **1**. The reaction of [HDMAN]**2** with 1,8-bis(dimethylamino)naphthalene (DMAN) confirmed this trend. In the presence of water, **2** transformed into the adduct $[(C_6F_5)_3BO(H)H\cdots O(H)B(C_6F_5)_3]^-$ (**3**), containing the borate **1** hydrogen-bonded to a water molecule coordinated to $B(C_6F_5)_3$. The same compound is formed by treating $(C_6F_5)_3BOH_2$ with 0.5 equiv of a base. A competition study established that for **1** the Lewis acid–base interaction with $B(C_6F_5)_3$ is about 5 times preferred over H-bonding to $(C_6F_5)_3BOH_2$. The X-ray single-crystal analysis of [2-methyl-3*H*-indolium]**3** provided the first experimental observation of an asymmetric H-bond in the $[H_3O_2]^-$ moiety, the measured O–H and H···O bond distances being significantly different [1.14(2) vs 1.26(2) Å]. The reaction of NEt_3 with an equimolar mixture of $B(C_6F_5)_3$ and bis(pentafluorophenyl)borinic acid, $(C_6F_5)_2BOH$, afforded the novel borinatoborate salt $[NHEt_3]^+[(C_6F_5)_3BOB(C_6F_5)_2]^-$ ($[NHEt_3]$**4**). X-ray diffraction showed that the B–O bond distances are significantly shorter than in $[(C_6F_5)_3B(\mu\text{-}OH)B(C_6F_5)_3]^-$. Variable-temperature ^{19}F NMR revealed high mobility of the five aryl rings, at variance with the more crowded anion **2**. 2D NMR correlation experiments showed that in CD_2Cl_2 the two anions $[(C_6F_5)_3BOH]^-$ and $[(C_6F_5)_3BH]^-$ form tight ion pairs with $[NHEt_3]^+$, in which the NH proton establishes a conventional (BO···HN) or an unconventional (BH···HN), respectively, hydrogen bond with the anion. The diborate anions **2**–**4**, on the contrary, gave loose ion pairs with the ammonium cation, due both to the delocalized anionic charge and to the more sterically encumbered position of the oxygen atoms that should act as H-bond acceptors.

Introduction

Perfluorinated aryl boron and borate compounds are being widely studied as stoichiometric activators of single-center olefin polymerization catalysts.[1] Recently, some attention has been devoted to the synthesis of delocalized polyborate anions, where two (or more) tris(pentafluorophenyl)borane molecules are coordinated to linking units such as pyrazolate,[2] NH_2^-,[3] CN^-,[4] or $[Ni(CN)_4]^{2-}$.[4] In these anions the negative charge is delocalized over more than one B atom,

* Authors to whom correspondence should be addressed. E-mail: luigi.resconi@basell.com (L.R.); giuseppe.dalfonso@unimi.it (G.D.); pierluigi.mercandelli@unimi.it (P.M.).
[†] Basell Polyolefins Italia.
[‡] Dipartimento di Chimica Inorganica, Metallorganica e Analitica, Facoltà di Farmacia, Università degli Studi di Milano.
[§] Dipartimento di Chimica Strutturale e Stereochimica Inorganica, Università degli Studi di Milano.

(1) (a) Chen, E. Y.-X.; Marks, T. J. *Chem. Soc. Rev.* **2000**, *100*, 1391. (b) Krossing, I.; Raabe, I. *Angew. Chem., Int. Ed.* **2004**, *43*, 2066. (c) Piers, W. E. *Adv. Organomet. Chem.* **2005**, *52*, 1.
(2) LaPointe, R. E.; Roof, G. R.; Abboud, K. A.; Klosin, J. *J. Am. Chem. Soc.* **2000**, *122*, 9560.
(3) Lancaster, S. J.; Rodriguez, A.; Lara-Sanchez, A.; Hannant, M. D.; Walker, D. A.; Hughes, D. H.; Bochmann, M. *Organometallics* **2002**, *21*, 451.

10.1021/ic0502168 CCC: $30.25
Published on Web 06/17/2005

Table 1. ^{1}H NMR Data of the $NHEt_3^+$ Salts of Anions **1**−**4** (CD_2Cl_2)

	T (K)	δ(OH)	δ(NH)	δ(C_2H_5)
[$NHEt_3$]**1**[a]	263	2.98	10.51 (s br)	2.84 (dq, CH_2, $^3J_{HH}$ = 7.0 Hz, $^3J_{HH}$ = 4.9 Hz) 1.14 (t, CH_3, $^3J_{HH}$ = 7.0 Hz)
[$NHEt_3$]**2**	223	6.58 t (J_{HF} = 17 Hz)	5.04 ($^1J_{HN}$ = 51 Hz)	3.27 (dq, CH_2, J_{HH} = 7.0 Hz) 1.34 (t CH_3)
[$NHEt_3$]**3**	298	8.49	5.04 ($^1J_{HN}$ = 53 Hz, $^3J_{HH}$ = 5.5 Hz)	3.36 (dq, CH_2, $^3J_{HH}$ = 7.3 Hz, $^3J_{HH}$ = 5.5 Hz)
	173	17.91 (s, 1H), 4.54 (s, 2H)	5.14 (s br)	1.47 (t, CH_3, $^3J_{HH}$ = 7.3 Hz) 3 0.28 (m, CH_2) 1.84 (t, CH_3, $^3J_{HH}$ = 6.9 Hz)
[$NHEt_3$]**4**	298		4.89 ($^1J_{HN}$ = 54 Hz, $^3J_{HH}$ = 5.3 Hz)	3.36 (dq, CH_2, $^3J_{HH}$ = 7.3 Hz, $^3J_{HH}$ = 5.3 Hz) 1.46 (t, CH_3, $^3J_{HH}$ = 7.3 Hz)

[a] Lit.[28] ^{1}H NMR ($CDCl_3$, room temperature): δ 11.04 (s, br, NH), 2.91 (q, 6H, NCH_2), 2.47 (s, 1H, BOH), 1.21 (t, 9H, CH_3).

Table 2. ^{19}F NMR Data of the $NHEt_3^+$ Salts of Anions **1**, **2**, **3** and **4** (CD_2Cl_2)

	T (K)	*ortho*	*para*	*meta*
$[B(C_6F_5)_3OH]^-$ (**1**)	223	−136.29	−160.27	−165.07
$[(C_6F_5)_3B(\mu\text{-}OH)B(C_6F_5)_3]^-$ (**2**)	173[a]	−129.72 (A2)	−157.34 (A4)	−162.57 (C3)
		−131.06 (A6)	−157.91 (C4)	−164.18 (C5)
		−131.58 (B2)	−159.23 (B4)	−164.32 (B5)
		−133.13 (C2)		−164.95 (A3)
		−137.93(C6)		165.20 (A5)
		−140.31 (B6)		−165.57 (B3)
$[(C_6F_5)_3BOH_2\cdots O(H)B(C_6F_5)_3]^-$ (**3**)	173	−136.30	−159.04	−164.61
$[(C_6F_5)_3BOB(C_6F_5)_2]^-$ (**4**)	253	−134.11[b]	−154.37[b]	−163.49[b]
		−134.68[c]	−161.55[c]	−166.64[c]

[a] In parentheses are given the attributions to *ortho* (2, 6), *meta* (3, 5), and *para* (4) positions in the C_6F_5 rings A−C. [b] Signal of the borinato moiety. [c] Signal of the borate moiety.

providing improved stability and activation ability to the trityl or ammonium salts of the complex anions. Following our interest on the chemistry of $B(C_6F_5)_3$ with donor molecules,[5−7] and looking for even simpler molecules which could be prepared from a neutral source of potentially acidic protons (thus not requiring salt metathesis to generate the final activator), we have investigated (or reinvestigated) the synthesis and reactivity of $[(C_6F_5)_3B-O(H)_x-B(C_6F_5)_{2+x}]^-$ (x = 0, 1) delocalized anions, and report here the first results of such an investigation.

Results and Discussion

A. Synthesis and NMR Characterization of the Anion $[(C_6F_5)_3B(\mu\text{-}OH)B(C_6F_5)_3]^-$ (2). Such an anion was already known in the literature, and it had been structurally characterized with different counterions.[8−10] In all cases its formation was caused by deprotonation of $(C_6F_5)_3BOH_2$,[11] but no synthetic procedure was reported. Moreover, neither its chemistry nor its solution structure were discussed in any detail by the authors, the main subject of their works concerning the chemistry of other species (the cationic counterparts[9,10] or the adducts of $B(C_6F_5)_3$ with water).[8]

We have now prepared anion **2** as follows: the reaction of the $(C_6F_5)_3BOH_2$ adduct with 1 equiv of NEt_3 afforded quantitatively the ion pair $[NHEt_3]^+[B(C_6F_5)_3OH]^-$ ($NHEt_3$·**1**), which has been spectroscopically characterized (eq 1, L = NEt_3, Tables 1 and 2). Addition of 1 equiv of $B(C_6F_5)_3$ to the borate anion **1** resulted in the formation of the $[NHEt_3]^+$ salt of the dimeric anion $[(C_6F_5)_3B(\mu\text{-}OH)B(C_6F_5)_3]^-$ (**2**), whose NMR data are reported in Tables 1 and 2 (eq 2). An analogous two-step procedure using the "Proton Sponge" 1,8-bis(dimethylamino)naphthalene (DMAN) as the base afforded the $HDMAN^+$ salts of **1** and **2**.

$$(C_6F_5)_3BOH_2 + L \rightleftarrows [HL]^+[(C_6F_5)_3BOH]^- \quad (1)$$

$$[HL]^+[B(C_6F_5)_3OH]^- + B(C_6F_5)_3 \rightleftarrows [HL]^+[(C_6F_5)_3B(\mu\text{-}OH)B(C_6F_5)_3]^- \quad (2)$$

The low-temperature ^{19}F spectrum of anion **2** consists of fifteen signals (three for the *para* and six each for the *ortho* and *meta* fluorine atoms), indicating an idealized C_2 symmetry. The ^{19}F signals of the three unequivalent rings A−C have been assigned by a 2D ^{19}F COSY at 173 K (Figure 1a,b).

Dipolar and scalar correlations observed in 2D ^{19}F−^{19}F and ^{1}H−^{19}F experiments led to the solution structure depicted in Figure 2, which maintains the main features of the previously reported solid-state structures. Relevant points for establishing this conformation were the following. Strong cross-peaks due to scalar "through-space" coupling between A2 and B6, B2 and C2, and, slightly weaker, B6 and C6

(4) Lancaster, S. J.; Walker, D. A.; Thornton-Pett, M.; Bochmann, M. *Chem. Commun.* **1999**, 1533.
(5) (a) Guidotti, S.; Camurati, I.; Focante, F.; Angellini, L.; Moscardi, G.; Resconi, L.; Leardini, R.; Nanni, D.; Mercandelli, P.; Sironi, A.; Beringhelli, T.; Maggioni, D. *J. Org. Chem.* **2003**, *68*, 5445. (b) Bonazza, A.; Camurati, I.; Guidotti, S.; Mascellani, N.; Resconi, L. *Macromol. Chem. Phys.* **2004**, *205*, 319. (c) Focante, F.; Camurati, I.; Nanni, D.; Leardini, R.; Resconi, L. *Organometallics* **2004**, *23*, 5135.
(6) Beringhelli, T.; Maggioni, D.; D'Alfonso, G. *Organometallics* **2001**, *20*, 4927.
(7) (a) Maggioni, D.; Beringhelli, T.; D'Alfonso, G.; Resconi, L. *J. Organomet. Chem.* **2005**, *690*, 640. (b) Beringhelli T.; D'Alfonso G.; Maggioni, D.; Mercandelli P.; Sironi A. *Chem.*—Eur. J. **2005**, *11*, 650.
(8) Danopoulos, A. A.; Galsworthy, J. R.; Green, M. L. H.; Cafferkey, S.; Doerrer, L. H.; Hursthouse, M. B. *Chem. Commun.* **1998**, 2529.
(9) Cowley, A. H.; Macdonald, C. L. B.; Silverman, J. S.; Gorden, J. D.; Voigt, A. *Chem. Commun.* **2001**, 175.
(10) Stender, M.; Phillips, A. D.; Power, P. P. *Inorg. Chem.* **2001**, *40*, 5314.
(11) The easy deprotonation of $(C_6F_5)_3B{\cdot}OH_2$ by bases is in line with the strong acidity of the $(C_6F_5)_3B{\cdot}OH_2$ adduct.[12]

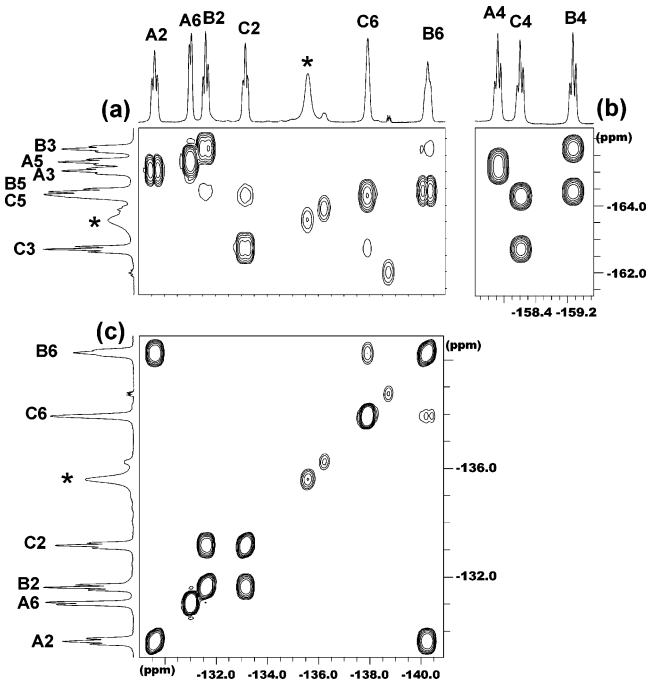

Figure 1. 2D ^{19}F COSYGS (173 K, 7.1 T) of a CD_2Cl_2 solution of $[(C_6F_5)_3BO(H)B(C_6F_5)_3]^-$ (**2**). The three aryl rings have been arbitrarily labeled as A, B, and C. Panels a and b show the correlations for the assignments; panel c shows the "through-space" scalar correlations in the *ortho* region. The asterisks mark the signals of $[(C_6F_5)_3BO(H)H\cdots O(H)B(C_6F_5)_3]^-$ (**3**), present as a byproduct.

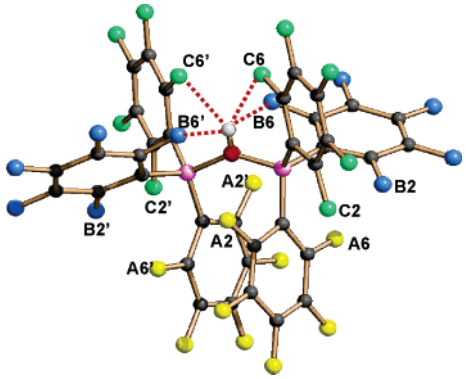

Figure 2. Solution structure of anion **2**, as inferred from the NMR 2D experiments.

were observed in the 2D ^{19}F COSY at 173 K (Figure 1c). Dipolar correlations between A2 and A6, A2 and C2, A6 and B2, and B6 and C6 were revealed by a 2D [^{19}F−^{19}F] NOESY at the same temperature. Moreover, the ^{1}H signal of the BOH proton (δ 6.5) exhibited through-space coupling with the two equivalent fluorine atoms C6 (δ −137.92) (see Figure 3 and the 2D ^{19}F−^{1}H COSY shown in Figure S1 of the Supporting Information) and dipolar correlations with six *ortho* fluorine atoms, namely, A2, B6, and C6 (see the 2D ^{19}F−^{1}H HOESY shown in Figure S2 of the Supporting Information).

Variable-temperature ^{1}H and ^{19}F spectra revealed the onset of dynamic processes. At T > 210 K all the ^{19}F signals broadened and then coalesced, resulting at room temperature in a single set of ^{19}F signals (one *ortho*, one *meta*, and one *para* resonance). This indicates the dynamic equivalence of the three aryl rings bonded to each boron atom and of the

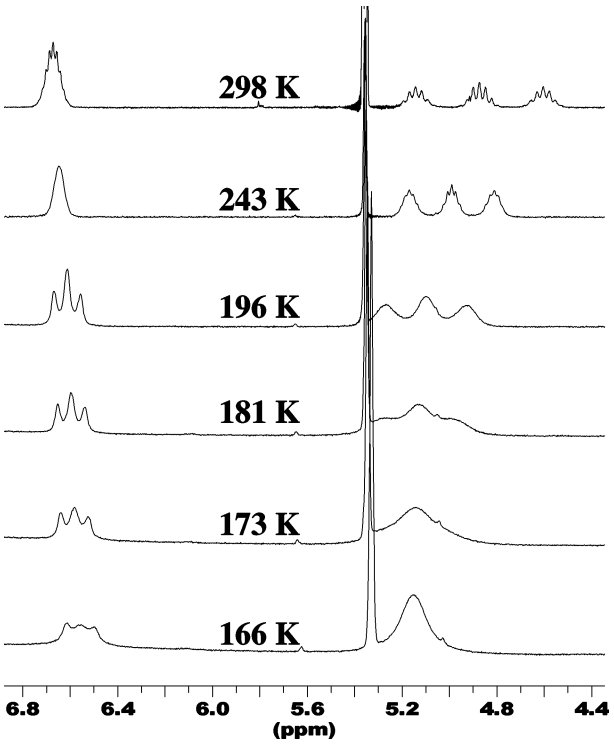

Figure 3. Low-field region of the variable-temperature ^{1}H NMR spectra of the $[NHEt_3]^+$ salt of anion **2** in CD_2Cl_2 solution. The room temperature trace was acquired at 4.7 T. The multiplet at ca. 5 ppm is due to the NH proton (see section E for the discussion of this signal).

ortho and *meta* positions within each ring. As a result of this dynamics, on increasing the temperature, the OH signal at 6.5 ppm changed its multiplicity (Figure 3) and passed from a triplet (196 K, with J_{HF} = 17 Hz) to a 13-line[13] multiplet, with averaged J_{HF} = ca. 3 Hz, indicative of the coupling of the OH proton with all twelve *ortho* fluorines in the six aryl rings. This pattern confirms that anion **2** contains a OH group bridging between two $B(C_6F_5)_3$ molecules.

More detailed information on the nature of these dynamic processes was provided by the correlations observed in the *meta* region[14] of a ^{19}F NOESY/EXSY experiment at 183 K (Figure 4), which showed the occurrence of two different enantiomerization processes for anion **2**. The first process exchanges rings B with rings C (e.g., in the *meta* region selective B3 ↔ C3 and B5 ↔ C5 interconversion, Figure 4b) through small oscillations occurring around their B−C_{ipso} interactions and simultaneous oscillations (in opposite directions) around the two B−O bonds. These small movements do not break the four hydrogen-bond interactions C6···HO (C6′···HO) and B6···HO (B6′···HO), but only cause their interchange. Rings A just shift from one side to the other of

(12) Bergquist, C.; Bridgewater, B. M.; Harlan, C. J.; Norton, J. R. *J. Am. Chem. Soc.* **2000**, *122*, 10581.

(13) Even if nine lines only were detectable in this multiplet, the experimental intensity ratio between these components corresponded well to the theoretical 0.015:0.18:1:3.3:7.5:12:14:12:7.5:3.3:1:0.18:0.015 ratio (Figure S3). The observed averaged J_{HF} corresponded well to the expected value, i.e., (17 × 2)/12.

(14) The nature of the exchange processes has been deduced mainly on the basis of the correlations in the *meta* region, since the cross-peaks in the *ortho* region were affected also by dipolar and scalar contributions, and the *para* region is intrinsically less informative.

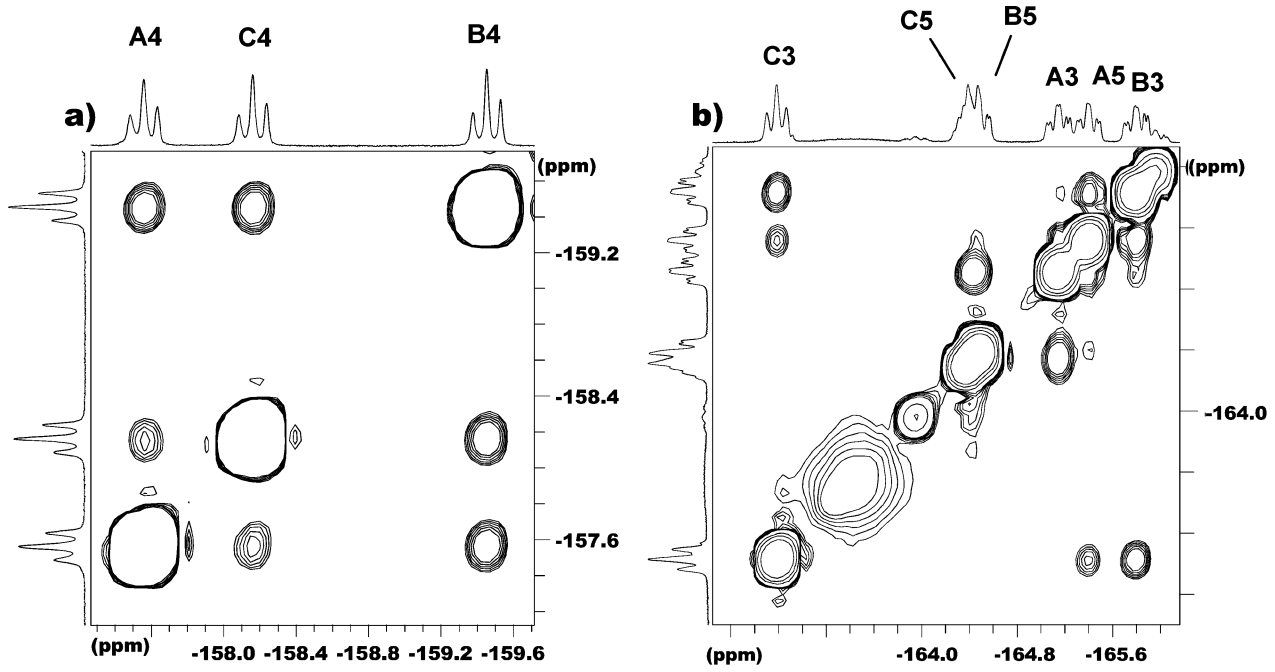

Figure 4. *Para* and *meta* regions of a [^{19}F−^{19}F] EXSY experiment on [NHEt$_3$]**2** (CD_2Cl_2, 183 K, mixing time 0.1 s).

the BO(H)B plane (see A3 ↔ A5 exchange), without any oscillation around their B−C_{ipso} bond.

The second process exchanges rings A and B (selectively A5 ↔ B3 and A3 ↔ B5, Figure 4b) by wider simultaneous oscillations around the B−O bond and around all six B−C_{ipso} interactions, to restore the propeller-like conformation. These oscillations cause the B6···HO and B6′···HO interactions to be broken, while C6···HO and C6′···HO interactions are maintained. Indeed, rings C just move from one side to the other of the BO(H)B plane, maintaining their identity.

The A/C exchange peaks (A3 ↔ C5, A5 ↔ C3, the first one partially overlapped with the A3 ↔ B5 exchange cross-peak, Figure 4b) are a consequence of the two above processes (A ↔ B ↔ C). Indeed, the volume analysis of the cross-peaks in the *para* and *meta* regions indicated that, while the two processes exchanging B/C and A/B rings have similar rates [$k_{BC} = 0.71$ s^{-1} from the *para* cross-peaks of Figure 4a and 0.73 s^{-1} from the *meta* cross-peaks; $k_{AB} = 0.65$ s^{-1} (*para*) and 0.64 s^{-1} (*meta*)], the indirect A/C exchange was about half those concerning the B/C and A/B exchanges [$k_{AC} = 0.38$ s^{-1} (*para*) and 0.34 s^{-1} (*meta*)], in agreement with the kinetic theory for this particular exchange.[15]

B. Reactions of 2 with NEt$_3$ and DMAN. We reasoned that B(C_6F_5)$_3$ coordination to the borate oxygen atom might provide some acidic character to the oxydrilic hydrogen atom, allowing its abstraction by a suitable base. However, attempts to deprotonate **2** with NEt$_3$ resulted in the reaction process depicted in Scheme 1.

(15) This system can be assimilated to a reversible two-step A ↔ B ↔ C reaction, in which the direct and the reverse kinetic constants in each step are equal. Moreover, in the present case, the kinetic constant from A to B is equal to that from C to B. In these hypotheses the kinetic constant for the A−C conversion should be half that for the A−B conversion: Bernasconi, C. F. Investigation of rates and Mechanisms of Reactions. In *Techniques of Chemistry*, 4th ed.; Weissemberger, A., Ed.; Wiley-Interscience Publishers: New York, 1986; Vol. VI, Part I, Chapter VI, p 449.

Scheme 1

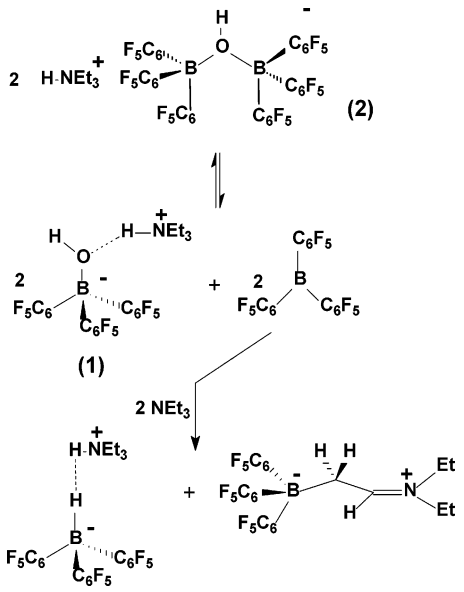

The identification of the reaction products (see the Experimental Section) has been greatly facilitated by a recent study concerning the reaction between B(C_6F_5)$_3$ and the tertiary amine NEt_2Ph,[16] which afforded the zwitterionic adduct (C_6F_5)$_3$B$^-$($CH_2CH{=}N^+EtPh$) and the ion pair [$NHEt_2Ph$]$^+$[(C_6F_5)$_3$BH]$^-$. In our case, the B(C_6F_5)$_3$ source is anion **2**, as depicted in Scheme 1. Indeed, we have verified that the reaction of B(C_6F_5)$_3$ with stoichiometric NEt$_3$ resulted in the instantaneous formation (even at low temperature, 193 K) of the same products as those obtained from anion **2** (eq 3).

$$2B(C_6F_5)_3 + 2NEt_3 \rightleftarrows [NHEt_3]^+[(C_6F_5)_3BH]^- + (C_6F_5)_3B^-(CH_2CH{=}N^+Et_2) \quad (3)$$

Scheme 2

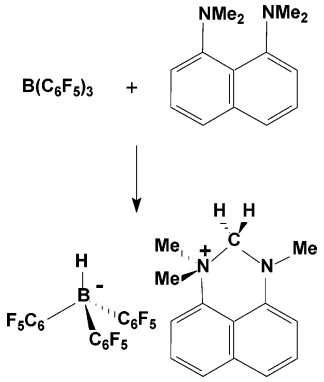

Scheme 3

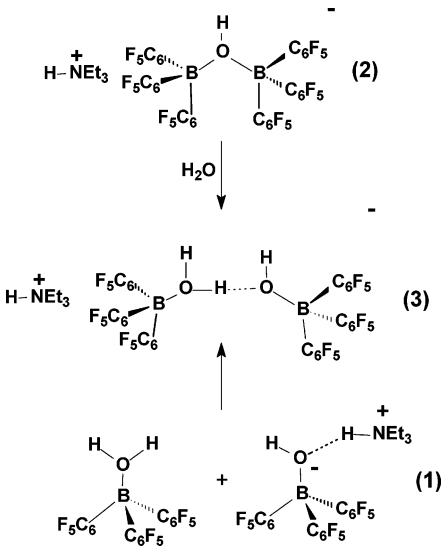

So the $B(C_6F_5)_3-NEt_3$ interaction does not afford a stable Lewis acid−base adduct,[17] but rather results in a formal hydride abstraction. Actually, even if a number of stable adducts are known between $B(C_6F_5)_3$ and neutral bases containing sp^2 or sp nitrogen atoms (such as imines,[18] aromatic heterocycles,[5,19] or cyano derivatives[19c]), the reports concerning adducts with sp^3 amines are much more scanty. It has recently been shown that $B(C_6F_5)_3$ adducts with the *sec*-amines pyrrolidine and piperidine are stable,[5,20] while the corresponding adduct with the tertiary amine NEt_2Me is stable only at low temperature, because at room temperature significant generation of an iminium salt of $[B(C_6F_5)_3H]^-$ was observed, as mentioned above.[16]

The failure of NEt_3 to deprotonate anion **2** prompted us to try the use of a stronger Brønsted base, such as the Proton Sponge DMAN. However, no deprotonation of **2** was observed, but rather reaction 4, in which $B(C_6F_5)_3$ reacts with DMAN (Scheme 2) to give the 1,1,3-trimethyl-2,3-dihydroperimidin-1-ium cation, $[(C_{10}H_6)(CH_3)_2N(CH_2)N(CH_3)]^+$ (TMP^+), previously structurally characterized.[21]

$$[HDMAN]^+[(C_6F_5)_3B(\mu\text{-}OH)B(C_6F_5)_3]^- + DMAN \rightleftarrows [HDMAN]^+[(C_6F_5)_3BOH]^- + [TMP]^+[(C_6F_5)_3BH]^- \quad (4)$$

C. Reaction of 2 with Water: The Anion $[(C_6F_5)_3BO(H)H\cdots O(H)B(C_6F_5)_3]^-$ (3). The NMR spectra of the reaction mixtures arising from $B(C_6F_5)_3$ addition to the $NHEt_3^+$ salt of the anion $[B(C_6F_5)_3OH]^-$ (**1**) always showed, besides anion **2**, also another minor component. Such a species has been identified as the ion pair $[NHEt_3]^+[(C_6F_5)_3BO(H)H\cdots O(H)B(C_6F_5)_3]^-$ ($[NHEt_3]$**3**), containing the borate anion **1** hydrogen-bonded to a proton of one water molecule coordinated to $B(C_6F_5)_3$, as shown in Scheme 3. The formation of this species is due to the presence of traces of water, both in the solvent and/or in the reactants, which transforms part of $B(C_6F_5)_3$ into its stable water adduct, $(C_6F_5)_3BOH_2$. This has been confirmed by the observation that water addition to the reaction mixtures increased the amount of **3** at the expense of **2** (see Scheme 3, top).

Anion **3** has been obtained in high yields also by treating the $(C_6F_5)_3BOH_2$ adduct with 0.5 equiv of NEt_3, according to reaction 1 (L = NEt_3) *plus* reaction 5. The process has been monitored in an NMR tube and afforded spectroscopically pure $[NHEt_3]$**3**. Reaction 5 is reminiscent of the reaction of anion **1** with the $[Tp'Zn(OH_2)]^+$ cation (Tp′ = substituted trispyrazolylborate), where **1** did not displace the coordinated water molecule, but rather gave a hydrogen bond with the water protons, affording a B-bound $H_3O_2^-$ anion.[23]

$$[NHEt_3]^+[(C_6F_5)_3BOH]^- + B(C_6F_5)_3OH_2 \rightleftarrows [NHEt_3]^+[(C_6F_5)_3BO(H)H\cdots O(H)B(C_6F_5)_3]^- \quad (5)$$

Interestingly, also the reaction of $(C_6F_5)_3BOH_2$ with 0.5 equiv of 2-methylindole afforded anion **3** in high yields, according to eq 6. A solid-state X-ray diffractometric analysis of the reaction product has been performed, providing a detailed characterization of the $H_3O_2^-$ moiety in the adduct (see section F). The 1:1 reaction between the same reactants

$$C_9H_9N + 2B(C_6F_5)_3OH_2 \rightleftarrows [C_9H_{10}N]^+[(C_6F_5)_3BO(H)H\cdots O(H)B(C_6F_5)_3]^- \quad (6)$$

(16) Millot, N.; Santini, C. C.; Fenet, B.; Basset, J. M. *Eur. J. Inorg. Chem.* **2002**, 3328.

(17) A $(C_6F_5)_3B{\cdot}NEt_3$ adduct has been previously briefly mentioned, but no detail of its behavior was given: (a) Doerrer, L. H.; Graham, A. J.; Haussinger, D.; Green, M. L. H. *Dalton Trans.* **2000**, 813. (b) Doerrer, L. H.; Graham, A. J., Green, M. L. H. *Dalton Trans.* **1998**, 3941.

(18) Blackwell, J. M.; Piers, W. E.; Parvez, M.; McDonald, R. *Organometallics* **2002**, *21*, 1400.

(19) (a) Lesley, M. J. G.; Woodward, A.; Taylor, N. J.; Marder, T. B.; Cazenobe, I.; Ledoux, I.; Zyss, J.; Thornton, A.; Bruce, D.; Kakkar, K. *Chem. Mater.* **1998**, *10*, 1355. (b) Vagedes, D.; Erker, G.; Kehr, G.; Bergander, K.; Kataeva, O.; Fröhlich, R.; Grimme, S.; Mück-Lichtenfeld, C. *Dalton Trans.* **2003**, 1337. (c) Fraenk, W.; Klapoetke, T. M.; Krumm, B.; Mayer, P.; Piotrowski, H.; Vogt, M. *Z. Anorg. Allg. Chem.* **2002**, *628*, 745.

(20) Mountford, A. J.; Hughes, D. L.; Lancaster, S. J. *Chem. Commun.* **2003**, 2148.

(21) Gamage, S. N.; Morris, R. H.; Rettig, S. J.; Thackray, D. C.; Thorburn, I. S.; James, B. R. *J. Chem. Soc., Chem. Commun.* **1987**, 894. In this work DMAN dehydrogenation was promoted by the complex *mer*-$RhCl_3(Me_2SO)_3$. The same Rh complex had been previously shown to easily dehydrogenate triethylamine with resulting formation of the ylidic imine complex $RhCl_3(Me_2SO)_2(CH_2CH{=}NEt_2)$.[22]

(22) Gamage, S. N.; Morris, R. H.; Rettig, S. J.; James, B. R. *J. Organomet. Chem.* **1986**, *309*, C59.

(23) (a) C. Bergquist G. Parkin, *J. Am. Chem. Soc.* **1999**, *121*, 6322. (b) Bergquist, C.; Fillebeen, T.; Morlok, M. M.; Parkin, G. *J. Am. Chem. Soc.* **2003**, *125*, 6189.

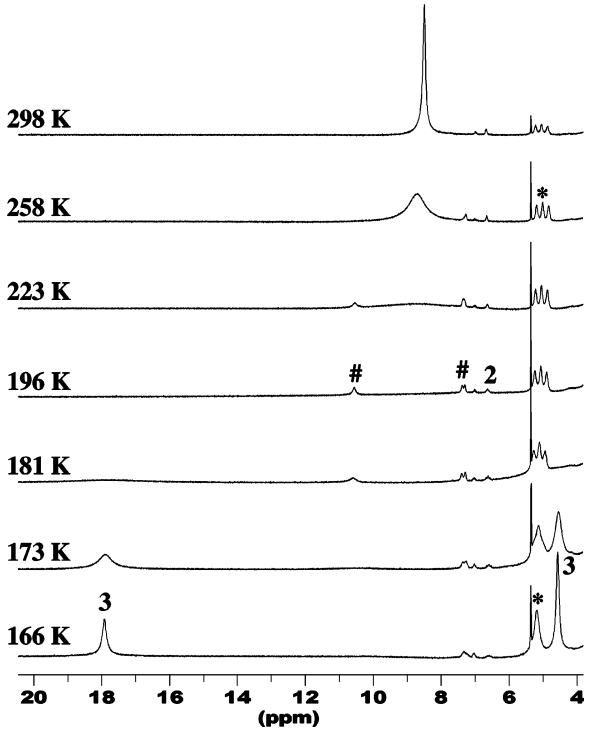

Figure 5. Low-field region of the variable-temperature ^{1}H NMR spectra of [NHEt$_3$]**3** in CD_2Cl_2. The asterisk marks the signal of the NH proton, while the pound sign indicates unidentified byproducts.

afforded the indolium salt of anion **1**, as described in the Experimental Section.

In CD_2Cl_2 solution, the room temperature ^{1}H spectrum of anion **3** consisted of a unique resonance, at δ 8.55. This indicates fast exchange among the three different protonic sites of the $H_3O_2^-$ moiety, i.e., the two water protons of $(C_6F_5)_3BOH_2$ and the proton of $(C_6F_5)_3BOH^-$. On lowering the temperature, the exchange slowed, causing broadening and collapse of the protonic resonance, eventually resulting in the appearance of two resonances at 17.9 and 4.5 ppm (ratio 1:2, Figure 5). The downfield position of the signal of intensity 1 indicates that this proton is involved in a very strong H-bonding interaction, and the 1:2 ratio indicates that such an interaction is (by itself or dynamically; see Scheme 4, top) symmetric. A possible mechanism for the hydrogen exchange could imply a partial breaking of the H-bond interaction, most likely with the intermediate formation of a bifurcated interaction, as shown in Scheme 4.

The ^{19}F NMR spectra showed one resonance only, for each of the *ortho*, *meta*, and *para* positions of the aryl rings (Figure 1). At $T < 223$ K, some broadening of the signals was observed, particularly for the *para* one, but no collapse was observed down to 166 K. This indicates that the fluxionality of the C_6F_5 rings, which equalizes the three aryls on each B atom and their *ortho* and *meta* positions, is fast on the NMR time scale even at 166 K, differently from what was observed for anion **2**. Therefore, the aryl rings in anion **3** enjoy a conformational freedom higher than that in **2**, due to the longer distance between the two $B(C_6F_5)_3$ moieties, which relieves inter-ring steric crowding and hinders the H···F hydrogen-bond interaction between the OH proton and the aryl substituents.

Scheme 4

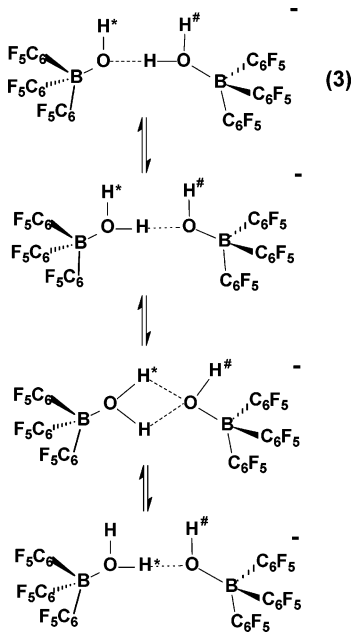

The borate anion **1** is therefore able to give adducts both with $B(C_6F_5)_3$ (eq 2) and with $(C_6F_5)_3BOH_2$ (eq 5). A competition study has been performed to establish the preferred reaction path. Mixtures containing $B(C_6F_5)_3/(C_6F_5)_3BOH_2$ in different ratios have been treated with NEt_3 (less than 1 equiv with respect to $(C_6F_5)_3BOH_2$), and the resulting equilibrium mixtures analyzed by ^{19}F NMR, at 173 K. In these systems, ^{1}H and ^{19}F averaged signals were observed for **3** and $(C_6F_5)_3BOH_2$, indicating fast exchange between the two species. Therefore, the relative amounts of **3** and of $(C_6F_5)_3BOH_2$ in the equilibrium systems had to be evaluated from the chemical shift of their molar fraction weighted averaged ^{19}F signals (while the amounts of **2** and of $B(C_6F_5)_3$ were estimated directly from the integrated intensities of their signals). From these computations a value of 0.20(3) was estimated for the constant of equilibrium 7. Such a value

$$[(C_6F_5)_3B(\mu\text{-}OH)B(C_6F_5)_3]^- + B(C_6F_5)_3OH_2 \leftrightarrow [(C_6F_5)_3BO(H)H\cdots O(H)B(C_6F_5)_3]^- + B(C_6F_5)_3 \quad (7)$$

corresponds to the ratio between the constants of equilibria 5 and 2 (with L = NEt_3). This indicates that for the borate **1** the Lewis acid−base interaction with $B(C_6F_5)_3$ (resulting in anion **2**) is about 5 times preferred over H-bonding to $(C_6F_5)_3BOH_2$ (resulting in **3**).

D. Synthesis and NMR Characterization of the Anion $[(C_6F_5)_3BOB(C_6F_5)_2]^-$ (4). As described in section B, it was not possible to obtain the dianion $[(C_6F_5)_3BOB(C_6F_5)_3]^{2-}$ by treating the salts of **2** with bases such as NEt_3 or DMAN. Nonetheless, we have been able to obtain a species containing the nonprotonated B−O−B moiety, by the reaction of NEt_3 with an equimolar mixture of $B(C_6F_5)_3$ and bis(pentafluorophenyl)borinic acid, $(C_6F_5)_2BOH$.[24,25] In this way the

(24) Chambers, R. D.; Chivers, T. *J. Chem. Soc.* **1965**, 3933.
(25) Beringhelli, T.; D'Alfonso, G.; Donghi, D.; Maggioni, D.; Mercandelli, P.; Sironi, A. *Organometallics* **2003**, *22*, 1588.

Scheme 5

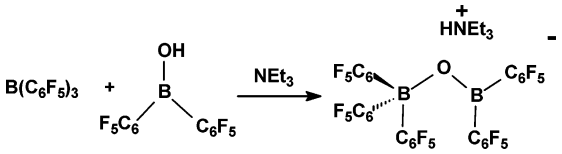

borinatoborate salt $[NHEt_3]^+[(C_6F_5)_3BOB(C_6F_5)_2]^-$ ([NHEt$_3$]-**4**) has been obtained in quantitative yield (Scheme 5). The solid-state structure is described in section F.

The ^{19}F NMR spectrum of **4** showed at all the temperatures two sets of resonances (of relative intensity 3:2) attributable to the $B(C_6F_5)_3$ and $B(C_6F_5)_2$ moieties of the anion, respectively. All the signals of the $B(C_6F_5)_3$ fragment were upfield shifted with respect to those of the $B(C_6F_5)_2$ fragment, in line with a higher electron density on tetracoordinated boron centers. On lowering the temperature, the resonances lost their fine structure and broadened, but even at 178 K no collapse was observed. This indicates higher mobility of the five aryl rings, compared to the more crowded anion **2**.

The sequence of reactant addition is crucial for the reaction depicted in Scheme 5. Indeed, NEt_3 reacts with $B(C_6F_5)_3$, according to reaction 3, and reactions occur also between NEt_3 and $(C_6F_5)_2BOH$ alone, affording complex mixtures that are presently under investigation. Therefore, we added NEt_3 to an equimolar mixture of $B(C_6F_5)_3$ and borinic acid. We have clear evidence that no fast reaction takes place upon mixing $B(C_6F_5)_3$ and $(C_6F_5)_2BOH$ (the only reaction that occurs is the very slow formation of the$(C_6F_5)_2BOB(C_6F_5)_2$ anhydride, by water removal due to the formation of the adduct of $B(C_6F_5)_3$ with water).[26] Therefore, we may suppose that the formation of **4** occurs by deprotonation of borinic acid and coordination of the $(C_6F_5)_2BO^-$ anion to the acidic boron atom of $B(C_6F_5)_3$, these steps having higher rates than reaction 3.

E. Different Nature of the Ion Pairs Containing $NHEt_3^+$, in CD_2Cl_2 Solution. In the ^1H spectrum the N−H signal of [NHEt$_3$]**1** was well downfield shifted with respect to that of the other ion pairs presented here (δ 10.5 vs 5.1). This is attributable to the occurrence of hydrogen bonding between the NH proton and the oxygen atom of the borate anion **1** (Scheme 1), as observed in the solid-state structure of the same ion pair.[27] Such a hydrogen bond makes [NHEt$_3$]-**1** a tight ion pair, and all the cationic signals of this ion pair were always separated from those of the other ion pairs, if present in the same reaction mixture.[30] The cation−anion spatial proximity was proved also by the dipolar correlations between the *ortho* fluorines and the cationic C_2H_5 resonances observed in a 2D $^{19}F-^1H$ HOESY at 173 K (Figure S5 of the Supporting Information).

In the case of [NHEt$_3$]**4** a low-temperature 2D $^{19}F-^1H$ HOESY (Figure S6) showed weak correlations between the *ortho* fluorine atoms of the anion and the C_2H_5 resonances of the cation (interestingly enough, stronger correlations were observed for the resonances of the $B(C_6F_5)_3$ moiety, in agreement with the electron density map described in Section F, Figure 9). Moreover, the N−H proton was observed at the usual chemical shift (δ 5.1), indicating the absence of significant $(C_6F_5)_3BO(R)\cdots HN$ hydrogen bonding. This is attributable to the higher steric crowding in **4** [R = $B(C_6F_5)_2$] than in **1** (R = H): the aryl rings effectively shield the oxygen atom toward the approach of the $NHEt_3^+$ cation.

In the case of ion pairs [NHEt$_3$]**2** and [NHEt$_3$]**3** low-temperature 2D experiments did not show any correlation between the cationic protons and the hydrogen or fluorine atoms of anions **2** and **3**. Moreover, a unique set of cationic resonances was observed, even at the lowest temperatures, in mixtures containing both [NHEt$_3$]**2** and [NHEt$_3$]**3**, indicating fast exchange between the cationic part of the ion pairs. These ion pairs should therefore be considered loose, due both to the higher delocalization of the anionic charge and to the lower propensity of the oxygen atoms to engage in a H-bond with the cation.

Finally, we have also investigated the nature of the ion pair $[NHEt_3]^+[(C_6F_5)_3BH]^-$, which is formed in the reaction of $B(C_6F_5)_3$ with NEt_3 (eq 3). In this case a 2D $^{19}F-^1H$ HOESY showed close proximity between all the cationic protons and the *ortho* fluorine atoms (see Figure S6 of the Supporting Information). This tight interaction is attributable to an unconventional hydrogen bond (a "dihydrogen bond")[31] involving the ammonium proton and the boron hydride, as revealed by the strong cross-peak between the corresponding resonances (at 6.2 and 3.4 ppm, respectively), observed in a ^{11}B-decoupled 2D NOESY (Figure 6).

The cationic NH resonance of the ion pairs with anions **2**−**4** (δ 5.1 ppm) shows the fine structure (pseudo 1:1:1 triplet, J_{HN} = 51 Hz) arising from the coupling with ^{14}N (in the spectra with the best resolution each triplet component is further split by the coupling with the six CH_2 protons). The observation of $^1H-^{14}N$ coupling is rather unusual and requires both the absence of proton exchange (typically with water traces) and relatively long quadrupolar ^{14}N relaxation times (at low temperatures the coupling disappeared, see Figures 3 and 5, due to the increase of the quadrupolar relaxation rate). This observation confirms that in these samples water is effectively trapped by $B(C_6F_5)_3$: indeed, the presence of traces of water destroyed the fine structure and modified the position of the signal, due to proton exchange.

F. Crystal and Molecular Structures of Anions 3 and 4 and Electrostatic Potential Maps for Anions 1−4. The structures of [2-methyl-3*H*-indolium]**3** and [NHEt$_3$]**4** have been determined in the solid state by X-ray diffraction analysis. Figures 7 and 8 show ORTEP drawings of anions

(26) Beringhelli, T.; D'Alfonso, G.; Donghi, D.; Maggioni, D.; Mercandelli, P.; Sironi, A. *Organometallics* **2004**, *23*, 5493.
(27) The solid-state X-ray structure of the $[NHEt_3]^+$ [28] (and also of the $[NHMe_2Ar]^+$)[29] salt of **1** showed a short N−O contact of ca. 273 pm.
(28) Duchateau, R.; Van Santen, R. A.; Yap, G. P. A. *Organometallics* **2000**, *19*, 809.
(29) Stibrany, R. T.; Brant, P. *Acta Crystallogr.* **2001**, *C57*, 644.
(30) Exchange with the $[NHEt_3]^+$ cation of the anions **2** and/or **3** does occur (as revealed by a cross-peak in the 2D EXSY map of Figure S4), but it is too slow to lead to averaged signals.
(31) (a) Custelcean, R.; Jacson, J. E. *Chem. Rev.* **2001**, *101*, 1963. (b) Crabtree, R. H.; Siegbahn, P. E. M.; Eisenstein, O.; Rheingold, A. L.; Koetzle, T. F. *Acc. Chem. Res.* **1996**, *29*, 348.

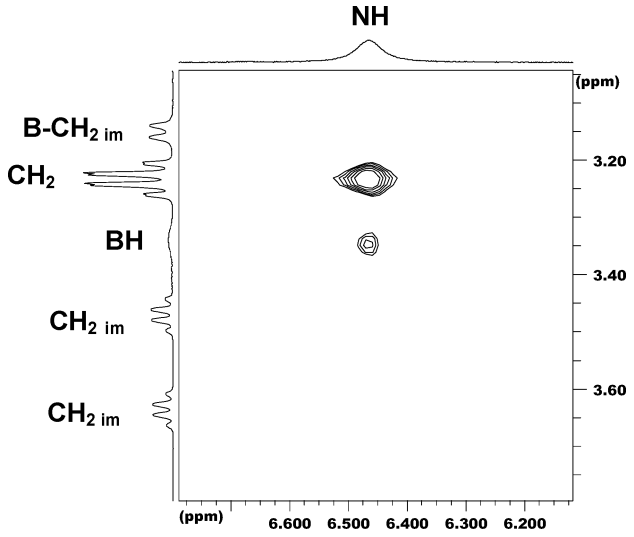

Figure 6. $\{^{11}B\}^1H-^1H$ NOESY experiment on a mixture containing the ion pair $[NHEt_3]^+[(C_6F_5)_3BH]^-$ and the zwitterionic imine $(C_6F_5)_3B^-(CH_2-CH{=}N^+Et_2)$, showing the proton−hydride NH···HB interaction (298 K, 9.4 T, mixing time 0.26 s). The signals of the imine are marked with the subscript "im".

3 and **4**, respectively. Tables 3 and 4 contain the most relevant bonding parameters for the two compounds.

Anion **3** consists of two triarylborane moieties bridged by a $[H_3O_2]^-$ anion, bound through the two oxygen atoms. Anion $[H_3O_2]^-$ has been extensively investigated theoretically to study its proton-transfer properties and as a prototypical strongly hydrogen bonded charged species.[32] Its computed geometry is strongly dependent on the model chemistry employed;[33] however, high-level correlated computations undoubtedly assign an asymmetric structure to the hydrogen bond.[34]

The solid-state structure of anion **3** can contribute to support these theoretical findings. Anion **3** has been previously structurally characterized as a salt of different cations; however, either it was impossible to properly locate hydrogen atoms[8] or the anion was constrained to lie on a crystallographic C_2 axis.[35] An accurate structural determination of [HDMAN]**3** has been recently published.[36] A distinct asymmetry of the overall anion was observed; however, the large estimated standard uncertainties affecting the OH bond distances hampered the direct assessment of the symmetric or asymmetric nature of the $[H_3O_2]^-$ moiety.

The geometry of anion **3** as determined in its 2-methyl-3*H*-indolium salt shows a clear deviation from the idealized C_2 symmetry, the observed bond distances and angles listed in Table 3 being consistent with an asymmetric structure for this species. Moreover, the measured O(1B)−H(1) and H(1)···O(1A) bond distances [1.14(2) and 1.26(2) Å] are significantly different and in fair agreement with the computed one for the free anion.[34]

Hydrogen atoms H(1A) and H(1B) are involved in bifurcated hydrogen bonds with two fluorine atoms each. In particular, H(1A) interacts with F(22A) of the same anion and with F(33B) of a symmetry-related anion ($-x$, $1-y$, $-z$), while H(1B) interacts with F(22B) of the same anion and with F(33A) of another symmetry-related anion ($-x$, $1-y$, $1-z$). Geometric parameters of these interactions are reported in Table 4.

The cation in $[C_9H_{10}N]$**3** is a rare example of the 3*H*-indole tautomeric form. Its structure compares well with the few previously reported: (3*H*-indole)tris(pentafluorophenyl)-boron[5] and $[PdCl_2(2\text{-methyl-}3H\text{-indole})_2]$.[37] The observed bond distances are in accordance with a localization of the double bond between N(1) and C(2) [1.271(3) Å] in the five-membered ring.

Anion $[(C_6F_5)_3B-O-B(C_6F_5)_2]^-$ (**4**) is the first borinatoborate structurally characterized. As expected, both the B−O bond distances are shorter in **4** than in the previously reported structures of $[(C_6F_5)_3B-OH-B(C_6F_5)_3]$ (**2**) (mean value 1.56 Å).[8−10] The observed B(2)−O(1) bond distance [1.306(2) Å] compares well with the values found in other borinic acid derivatives: 1.348 and 1.350 Å in $[(C_6H_5)_2BOH]$ and $[(2,4,6\text{-}(CF_3)_3C_6H_2)_2BOH]$, respectively.[38] A direct comparison with $[(C_6F_5)_2BOH]$ is hampered by the trimerization of this species in the solid state.[25] The B(1)−O(1) bond distance [1.496(2) Å] is unexceptional for $[(C_6F_5)_3BOX]$ derivatives; in particular it is similar to the value found in **3** [1.514(2) Å].

As can be seen from Figures 7 and 8 and from the torsional angles reported in Table 3, in the two anions the $B(C_6F_5)_3$ moiety adopts a very similar conformation in which one of the three phenyl rings [the one labeled C(11)−C(16)] eclipses the B−O bond, whereas the other two exhibit a chiral two-bladed propeller-like conformation. This very same conformation can be found in most of the crystal structures of tris(pentafluorphenyl)borane derivatives collected in the Cambridge Structural Database:[39] from this evidence it can be inferred that this molecular fragment is a very rigid one, so that the presence of a somehow high-energy barrier to the enantiomerization process of the chiral propeller can be expected.

As can be seen from the data in Table 4, the oxygen atoms in anions **3** and **4** are not involved in hydrogen bonding, the cation protons mainly interacting with the *ortho* fluorine atoms of the perfluorophenyl moieties. The very same situation has been found for the previously known structures of anions **2** and **3** with different counterions.[8−10,35,36] At variance, in the structure of $[NHEt_3]$**1** the oxygen atom acts as a hydrogen-bond acceptor for the cation.[28] These findings

(32) Tuckerman, M. E.; Marx, D.; Klein, M. L.; Parrinello, M. *Science* **1997**, *275*, 817.
(33) Wei, D.; Proynov, E. I.; Milet, A.; Salahub, D. R. *J. Phys. Chem. A* **2000**, *104*, 2384 and references therein.
(34) At the MP2(fc)/aug-cc-pVQZ level O−H and H···O bond distances are equal to 1.125 and 1.342 Å. Samson, C. C. M.; Klopper, W. *J. Mol. Struct.: THEOCHEM* **2002**, *586*, 201.
(35) Doerrer, L. H.; Green, M. L. H. *J. Chem. Soc., Dalton Trans.* **1999**, 4325.
(36) Drewitt, M. J.; Niedermann, M.; Baird, M. C. *Inorg. Chim. Acta* **2002**, *340*, 207.
(37) Yamauchi, O.; Takani, M.; Toyada, K.; Masuda, H. *Inorg. Chem.* **1990**, *29*, 1856.
(38) (a) Retting, S. J.; Trotter, J. *Can. J. Chem.* **1983**, *61*, 2334. (b) Fraenk, W.; Klapotke, T. M.; Krumm, B.; Mayer, P.; Noth, H.; Piotrowski, H.; Suter, M. *J. Flourine Chem.* **2001**, *112*, 73.
(39) CSD (version 5.24, November 2002). Allen, F. H. *Acta Crystallogr., Sect. B: Struct. Sci.* **2002**, *58*, 380.

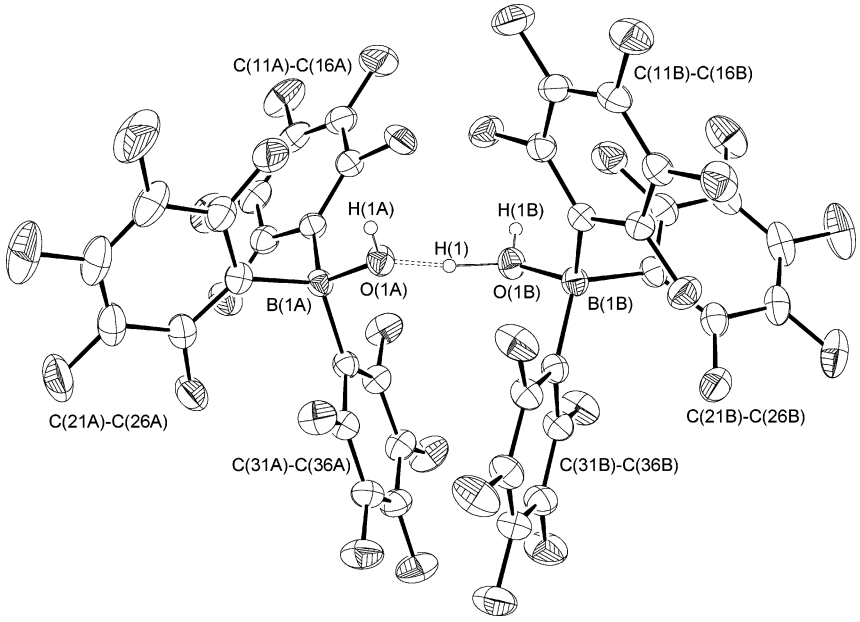

Figure 7. ORTEP view of the hydrogen-bonded adduct **3** between aquatris(pentafluorophenyl)borane and hydroxotris(pentafluorophenyl)borate, as determined in the crystal of its 2-methyl-3*H*-indolium salt. Thermal ellipsoids are drawn at the 30% probability level; hydrogen atoms are given arbitrary radii.

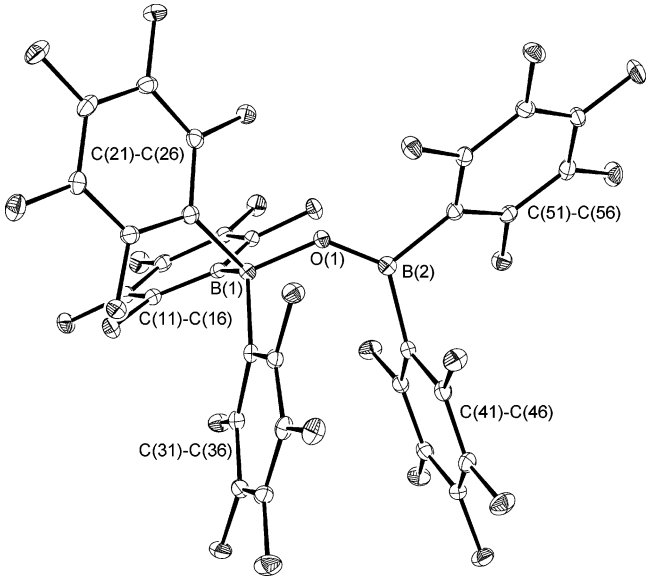

Figure 8. ORTEP view of the [bis(pentafluorophenyl)borinato]tris(pentafluorophenyl)borate anion (**4**), as determined in the crystal of its triethylammonium salt. Thermal ellipsoids are drawn at the 30% probability level.

closely parallel the NMR observations concerning the ion pair interactions in dichloromethane solution (see section E).

The limited accessibility of the oxygen atom in anions **2**−**4** with respect to **1** is clearly evidenced in Figure 9, in which the space-filling models of these species are depicted. In all cases, and particularly for anion **2**, the oxygen atom is buried inside the entangled arrangement of the perfluorophenyl rings. The situation is less severely hindered for anions **3** and **4**, this being reflected by the greater rotational freedom noticed in solution for these two anions.

However, in addition to these steric considerations, the tendency of diborates **2**−**4** to give looser ion pairs with respect to the borate **1** is attributable to the spreading of the anionic charge on a greater number of electronegative atoms: the electrostatic potential maps represented in Figure 9[40] show a considerable reduction of the negative potential on the oxygen atom *and* on the whole accessible surface of anions **2**−**4**, the charge being delocalized on all the fluorine atoms. Between the three diborate anions, the borinatoborate species **4** shows the largest local negative potential, due to the lower number of fluorine atoms among which the charge has to be distributed: the NMR evidence of a partial interaction of this species with the proton of the triethylammonium cation in solution agrees with these findings.

Conclusions

We have pursued the synthesis of diborate anions in the hypothesis that the delocalization of the negative charge over more than one boron atom might improve the stability of the anion and provide higher acidity to the ammonium salts of the complex anions. The results reported here give some support to this idea. Indeed, the dinuclear anions $[(C_6F_5)_3B(\mu\text{-}OH)B(C_6F_5)_3]^-$ (**2**) and $[(C_6F_5)_3B(\mu\text{-}O)B(C_6F_5)_2]^-$ (**4**) form loose ion pairs and no evidence of the involvement of their ammonium cations in hydrogen bonds has been found, differently from the mononuclear anions $[(C_6F_5)_3BOH]^-$ (**1**) and $[(C_6F_5)_3BH]^-$. Therefore, the cations in the dinuclear ion pairs are expected to be more active toward nucleophiles.

On the other hand, the reaction of **2** with NEt_3 and DMAN indicates that reaction 2 is reversible, so that, in the presence of competing bases, **2** can dissociate, generating $B(C_6F_5)_3$ and $[(C_6F_5)_3BOH]^-$. Then anion **2** does not seem to be the ideal partner of the Brønsted acid $[NHEt_3]^+$, because it can behave as a source both of the competing Lewis acid $B(C_6F_5)_3$ and of the coordinating[41] anion $[(C_6F_5)_3BOH]^-$.

(40) The electrostatic potential was computed at the PM3 semiempirical level, employing the solid-state geometries. The calculations were performed with *SPARTAN 02*; Wavefunction Inc.: Irvine, CA, 2002.

(41) Hill, G. S.; Manojlovic-Muir, L.; Muir, K. W.; Puddephatt, R. J. *Organometallics* **1997**, *16*, 525

Table 3. Selected Geometric Parameters (Å,deg) for [2-Methyl-3*H*-indolium]**3** and [$NHEt_3$]**4**

[2-methyl-3*H*-indolium]**3**		[$NHEt_3$]**4**	
B(1A)−O(1A)	1.514(2)	B(1)−C(11)	1.652(2)
B(1A)−C(11A)	1.648(2)	B(1)−C(21)	1.661(2)
B(1A)−C(21A)	1.658(2)	B(1)−C(31)	1.650(2)
B(1A)−C(31A)	1.640(2)	B(1)−O(1)	1.496(2)
B(1B)−O(1B)	1.527(2)	B(2)−O(1)	1.306(2)
B(1B)−C(11B)	1.651(2)	B(2)−C(41)	1.615(2)
B(1B)−C(21B)	1.648(2)	B(2)−C(51)	1.600(2)
B(1B)−C(31B)	1.632(2)	C(11)−B(1)−C(21)	103.92(12)
N(1)−C(2)	1.271(3)	C(11)−B(1)−C(31)	116.57(13)
N(1)−C(7a)	1.430(3)	C(11)−B(1)−O(1)	110.54(13)
C(2)−C(3)	1.467(3)	C(21)−B(1)−C(31)	111.04(13)
C(2)−C(8)	1.479(4)	C(21)−B(1)−O(1)	107.18(12)
C(3)−C(3a)	1.495(3)	C(31)−B(1)−O(1)	107.25(13)
C(3a)−C(4)	1.379(3)	O(1)−B(2)−C(41)	126.53(15)
C(3a)−C(7a)	1.368(3)	O(1)−B(2)−C(51)	118.46(15)
C(4)−C(5)	1.363(5)	C(41)−B(2)−C(51)	114.96(13)
C(5)−C(6)	1.384(6)	B(1)−O(1)−B(2)	134.07(13)
C(6)−C(7)	1.377(6)	O(1)−B(1)−C(11)−C(12)	−6.9(2)
C(7)−C(7a)	1.346(4)	O(1)−B(1)−C(21)−C(22)	44.93(19)
O(1A)−B(1A)−C(11A)	112.50(12)	O(1)−B(1)−C(31)−C(32)	−119.37(17)
O(1A)−B(1A)−C(21A)	106.75(12)	O(1)−B(2)−C(41)−C(42)	78.1(2)
O(1A)−B(1A)−C(31A)	102.83(12)	O(1)−B(2)−C(51)−C(52)	−134.08(16)
C(11A)−B(1A)−C(21A)	105.55(12)		
C(11A)−B(1A)−C(31A)	113.13(12)		
C(21A)−B(1A)−C(31A)	116.07(13)		
O(1B)−B(1B)−C(11B)	112.46(12)		
O(1B)−B(1B)−C(21B)	106.80(12)		
O(1B)−B(1B)−C(31B)	102.64(12)		
C(11B)−B(1B)−C(21B)	104.48(12)		
C(11B)−B(1B)−C(31B)	115.08(12)		
C(21B)−B(1B)−C(31B)	115.32(13)		
C(2)−N(1)−C(7a)	113.2(2)		
N(1)−C(2)−C(3)	108.7(2)		
N(1)−C(2)−C(8)	123.3(3)		
C(3)−C(2)−C(8)	128.0(3)		
C(2)−C(3)−C(3a)	103.89(18)		
C(3)−C(3a)−C(4)	134.0(2)		
C(3)−C(3a)−C(7a)	107.3(2)		
C(4)−C(3a)−C(7a)	118.8(3)		
C(3a)−C(4)−C(5)	118.3(3)		
C(4)−C(5)−C(6)	121.8(3)		
C(5)−C(6)−C(7)	119.9(3)		
C(6)−C(7)−C(7a)	117.1(3)		
N(1)−C(7a)−C(3a)	106.9(2)		
N(1)−C(7a)−C(7)	129.0(3)		
C(3a)−C(7a)−C(7)	124.1(3)		
O(1A)−B(1A)−C(11A)−C(12A)	−3.9(2)		
O(1A)−B(1A)−C(21A)−C(22A)	48.36(19)		
O(1A)−B(1A)−C(31A)−C(32A)	−104.38(17)		
O(1B)−B(1B)−C(11B)−C(12B)	−8.5(2)		
O(1B)−B(1B)−C(21B)−C(22B)	48.18(18)		
O(1B)−B(1B)−C(31B)−C(32B)	−108.17(17)		

Table 4. Hydrogen-Bond Geometry (Å,deg) for [2-Methyl-3*H*-indolium]**3** and [$NHEt_3$]**4**[a]

D−H···A	D−H[a]	H···A	D···A	−D−H···A
[2-Methyl-3*H*-indolium]**3**				
O(1B)−H(1)···O(1A)	1.14(2)	1.26(2)	2.4040(16)	173(2)
O(1A)−H(1A)···F(22A)	0.80(3)	2.16(3)	2.7401(18)	128(2)
O(1A)−H(1A)···F(33B)^{i}	0.80(3)	2.23(3)	2.8977(17)	140(3)
O(1B)−H(1B)···F(22B)	0.78(3)	2.16(3)	2.7058(18)	128(2)
O(1B)−H(1B)···F(33A)^{ii}	0.78(3)	2.42(3)	3.0601(19)	140(2)
N(1)−H(N1)···F(12A)	0.991	1.998	2.940(2)	157.80
[$NHEt_3$]**4**				
N(1)−H(1)···F(56)	0.958	2.126	3.0246(19)	155.63

[a] Symmetry-equivalent positions: (i) $-x$, $1-y$, $-z$, (ii) $-x$, $1-y$, $1-z$.

Therefore, the novel borinatoborate anion **4**, despite its ion pair with $[NHEt_3]^+$ being slightly tighter than that of **2**, appears the most promising delocalized anion in this series, due to its higher stability toward dissociation. Studies aimed at further investigating its properties are in progress.

Experimental Section

General Procedures. All the manipulations were performed under nitrogen using oven dried Schlenk-type glassware. Deuterated solvents (CIL or Isotec Inc.) were anhydrified on activated molecular sieves. $B(C_6F_5)_3$ (Boulder Scientific Co.) and DMAN (Aldrich) were used as received. $(C_6F_5)_2BOH$ was provided by Basell GmbH. Triethylamine (Aldrich) was dried over KOH pellets and stored over activated 4 Å molecular sieves before use. $(C_6F_5)_3BOH_2$ was synthesized as reported in a previous paper.[5]

NMR spectra were acquired on Bruker spectrometers: DPX 200 for ^{13}C and ^{11}B spectra at room temperature, AVANCE DRX-300 equipped with a 5 mm QNP probe for ^{1}H and ^{19}F spectra, and AVANCE DRX 400 for ^{1}H and ^{11}B spectra. ^{19}F NMR spectra were referenced to external $CFCl_3$ ($\delta = 0$ ppm) and ^{11}B NMR spectra to

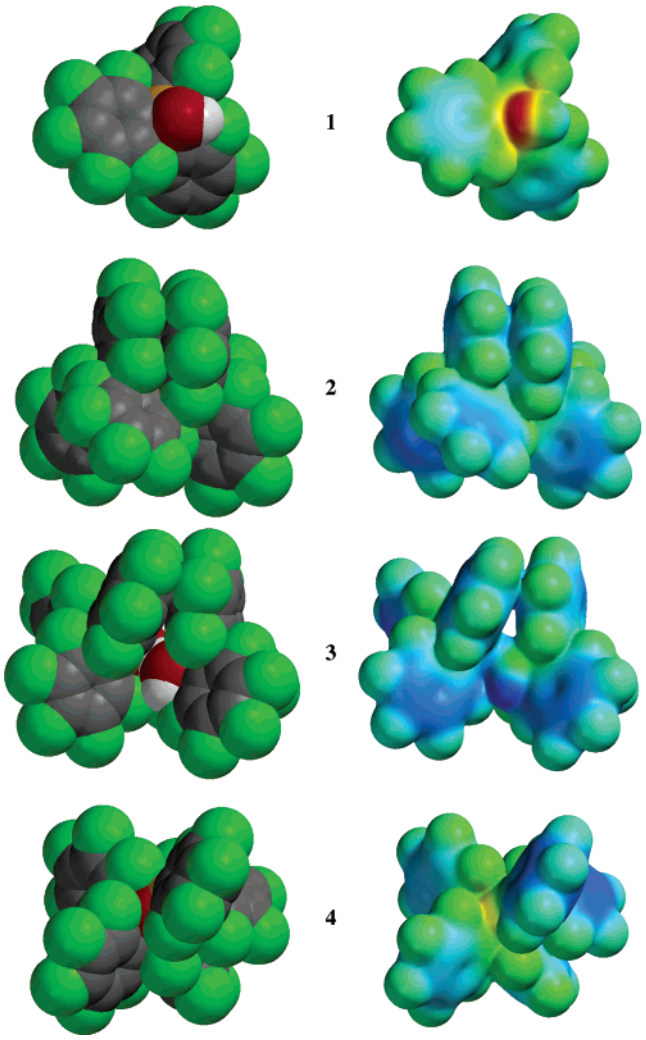

Figure 9. Space-filling models (left) and electrostatic potential mapped onto the electron density isosurfaces (0.002 au, right) for anions **1**−**4**. Dark red (blue) corresponds to −0.145 (−0.020) au.

external $Et_2O{\cdot}BF_3$ (δ = 0 ppm). The temperature was calibrated with a standard CH_3OH/CD_3OD solution.[42]

Preparation of $[NHEt_3]^+[B(C_6F_5)_3OH]^-$ ([NHEt$_3$]1). A CD_2Cl_2 solution of $B(C_6F_5)_3$ (26.7 mg, 0.0522 mmol) was treated directly in an NMR tube with H_2O up to exactly 1 equiv (as checked by low-temperature ^{19}F NMR) and then with 1 equiv (7.2 μL) of NEt_3. The low-temperature ^1H and ^{19}F data are reported in Table 1. The attribution to the NH proton of the signal at 10.51 ppm was confirmed by a COSY experiment (263 K). The identification of the OH signal was provided by a 2D NOESY (173 K), which showed correlation between the NH signal and a broad resonance almost overlapped with the CH_2 resonance, at 2.59 ppm. ^{11}B NMR (CD_2Cl_2, 298 K): δ −3.79 (br s) (lit.[43] δ −3.8 in $CDCl_3$, with the same counterion; lit.[41] δ −4.4, in CD_2Cl_2, with a different cation).

Preparation of $[NHEt_3]^+[(F_5C_6)_3B(\mu\text{-}OH)B(C_6F_5)_3]^-$ ([NHEt$_3$]2). A slightly beige and cloudy CH_2Cl_2 solution of $(C_6F_5)_3BOH_2$ (0.3626 g, 0.684 mmol) was treated with a CH_2Cl_2 solution of NEt_3 (0.0693 g, 99.5%, 0.685 mmol), reaching a total volume of 8 mL (0.085 M). Then 7 mL of a CH_2Cl_2 solution of $B(C_6F_5)_3$ (0.3499 g, 0.683 mmol) was added to the reaction mixture. Neither color variations nor exothermicity was observed. After 15 min a sample was evaporated to dryness and analyzed by ^1H NMR, showing quantitative formation of [NHEt$_3$]**2**. ^1H and ^{19}F NMR data are reported in Tables 1 and 2. ^{11}B NMR (CD_2Cl_2, 298 K): δ −0.63.

Reaction of $B(C_6F_5)_3$ with NEt_3. A CD_2Cl_2 solution of $B(C_6F_5)_3$ (30.6 mg, 0.0598 mmol) was treated directly in an NMR tube with 0.95 equiv of NEt_3 (7.9 μL) at 193 K. ^1H and ^{19}F NMR spectra were then acquired at different temperatures, showing the quantitative formation of an equimolar mixture of $[NHEt_3]^+[(C_6F_5)_3BH]^-$ and $(C_6F_5)_3B^-(CH_2CH{=}N^+Et_2)$. ^{19}F and ^1H assignments have been performed through $^{19}F-^1H$ HOESY and $^1H-^1H$ NOESY experiments, respectively. The hydrogen of the anion $[(C_6F_5)_3BH]^-$ has been detected in a $\{^{11}B\}^1H$ spectrum (3.33 ppm), the four lines of its multiplet (J_{BH} = 89 Hz) being otherwise largely buried under the methylene resonances. The following are data for $(C_6F_5)_3B^-(CH_2CH{=}N^+Et_2)$, in CD_2Cl_2 at 298 K. ^1H NMR (CD_2Cl_2, 298 K): δ 1.23 (t, 3H, C*H*$_3$ *anti* with respect to CH, $^3J_{HH}$ = 7.2 Hz), 1.25 (t, 3H, C*H*$_3$ *syn* with respect to CH, $^3J_{HH}$ = 7.35 Hz), 3.15 (br m, 1H, C*H*$_2$; d in $\{^{11}B\}^1H$, $^3J_{HH}$ = 8.0 Hz), 3.47 (q, 2H, C*H*$_2$ *anti* with respect to CH, $^3J_{HH}$ = 7.2 Hz), 3.63 (q, 2H, C*H*$_2$ *syn* with respect to CH, $^3J_{HH}$ = 7.35 Hz), 8.05 (t, 1H, N=C*H*, $^3J_{HH}$ = 8.0 Hz). ^{19}F NMR: δ −132.84 (m, 6F$_{ortho}$), −160.65 (m, 3F$_{para}$), −165.29 (m, 6F$_{meta}$). ^{11}B NMR (CD_2Cl_2, 298 K): δ −14.04 (pseudo s). The following are data for $[NHEt_3]^+[(C_6F_5)_3BH]^-$, in CD_2Cl_2 at 298 K. $\{^{11}B\}^1H$ NMR: δ 1.35 (t, 9H, C*H*$_3$, $^3J_{HH}$ = 7.3 Hz), 3.26 (q, 6H, C*H*$_2$, $^3J_{HH}$ = 7.4 Hz), 3.33 (br s, 1H, B*H*), 6.48 (br s, 1H, N*H*). ^{19}F NMR: δ −134.76 (m, 6F$_{ortho}$), −162.79 (m, 3F$_{para}$), −166.48 (m, 6F$_{meta}$). ^{11}B NMR: δ −24.40 (d, J_{BH} = 89 Hz).

Reaction of [NHEt$_3$]2 with NEt_3. A CD_2Cl_2 solution of [NHEt$_3$]-**2** (0.599 g, 5.24 mmol, 0.105 M) was treated with 1 equiv of NEt_3 (3.5 mL of a 1.5 M solution in CD_2Cl_2). Neither color variations nor exothermicity was observed. A sample was evaporated to dryness and analyzed by ^1H NMR, which showed the presence of $[NHEt_3]^+[(C_6F_5)_3BOH]^-$ as the main product (ca. 60%) together with an equimolar mixture of $[NHEt_3]^+[(C_6F_5)_3BH]^-$ and $(C_6F_5)_3B^-(CH_2CH{=}N^+Et_2)$.

Preparation of $[1\text{-}(Me_2NH)\text{-}8\text{-}(Me_2N)C_{10}H_6]^+[(C_6F_5)_3BOH]^-$ ([HDMAN]1). A CH_2Cl_2 (6 mL) suspension of $(C_6F_5)_3BOH_2$ (0.605 g, 1.14 mmol) was treated with 6 mL of a CH_2Cl_2 solution of DMAN (0.244 g, 1.14 mmol). A sample was evaporated to dryness and analyzed by ^1H NMR, showing the quantitative formation of [HDMAN]**1**. ^1H NMR (CD_2Cl_2, 298 K): δ 1.99 (br s, O*H*), 3.15 (d, 12H, C*H*$_3$, J_{HH} = 2.5 Hz), 7.7−8.1 (m, 6H, C*H*), 19.4 (pseudo br s, 1H, N*H*). ^{13}C NMR (CD_2Cl_2, 298 K, 4.7 T): δ 46.78 (*C*H$_3$), 121.53 (*C*H), 127.67 (*C*H), 130.45 (*C*H), 143.48 (*C*$_{ipso}$). COSY (CD_2Cl_2): $\delta(^1H)/\delta(^1H)$ 3.15/19.3 (C*H*$_3$/N*H*).

Preparation of $[1\text{-}(Me_2NH)\text{-}8\text{-}(Me_2N)C_{10}H_6]^+[(C_6F_5)_3B(\mu\text{-}OH)B(C_6F_5)_3]^-$ ([HDMAN]2). A CH_2Cl_2 solution of [HDMAN]**1** (11.8 mL, 0.095 M) was treated with 1 equiv of $B(C_6F_5)_3$ (4.0 mL of a 0.28 M solution in CH_2Cl_2). A sample was evaporated to dryness and analyzed by ^1H NMR, showing the quantitative formation of [HDMAN]**2**. ^1H NMR (CD_2Cl_2, 298 K): δ 6.67 (m with 13 lines, O*H*, averaged J_{HF} = 3.1 Hz), 3.18 (d, 12H, C*H*$_3$, J_{HH} = 2.7 Hz), 7.7−8.1 (m, 6H, C*H*), 19.4 (pseudo br s, 1H, N*H*).

Reaction of $B(C_6F_5)_3$ with DMAN. A slightly beige suspension of $B(C_6F_5)_3$ (0.406 g, 0.793 mmol) in CH_2Cl_2 (5 mL) was treated with 5 mL of a CH_2Cl_2 solution of DMAN (0.170 g, 0.793 mmol). The reaction was instantaneous, producing a slightly yellow and clear solution containing $[(C_{10}H_6)(CH_3)_2N(CH_2)N(CH_3)]^+[(C_6F_5)_3BH]^-$. ^1H NMR (CD_2Cl_2, 298 K): δ 3.36 (s, 3H, C*H*$_3$), 3.57 (br s, 6H, C*H*$_3$), 3.68 (br q, 1H, B*H*, J_{BH} = 89 Hz), 4.76 (s, 2H, C*H*$_2$), 7.08 (dd, 1H, C*H*, J_{HH} = 1.76, 6.85 Hz), 7.6−7.8 (m, 4H, C*H*), 8.0−8.1 (m, 1H, C*H*). ^{11}B NMR (CD_2Cl_2, 298 K): δ

(42) Van Geet, A. L. *Anal. Chem.* **1970**, *42*, 679.
(43) Siedle, A. R.; Newmark, R. A.; Lamanna, W. M.; Huffman, J. C. *Organometallics* **1993**, *12*, 1491.

−25.25 (d, J_{BH} = 89 Hz). ^{13}C NMR ($C_2D_2Cl_4$, 298 K): δ 37.83 (N*C*H$_3$), 52.55 (N(*C*H$_3$)$_2$), 80.68 (*C*H$_2$), 110.9 (*C*H), 114.2 (*C*H), 121.2 (*C*H), 126.2 (*C*H), 129.4 (*C*H), 132.1 (*C*H), 135.3 (q), 138.8 (q).

Reaction of [HDMAN]2 with DMAN. A CH_2Cl_2 (16 mL) solution of [HDMAN]**2** (1.11 mmol) was treated with 4 mL of a CH_2Cl_2 solution of DMAN (0.237 g, 1.11 mmol). Neither color variations nor exothermicity was observed. After 3 days ^{1}H NMR analysis showed the presence mainly of [HDMAN]**1** (49.3%) and [1,1,3-trimethyl-2,3-dihydro-1*H*-perimidin-1-ium]$^+$[HB(C$_6$F$_5$)$_3$]$^-$ (32.8%), together with some unreacted [HDMAN]**2** (9.4%) and DMAN (8.5%).

Reaction of 2-methylindole with (C$_6$F$_5$)$_3$BOH$_2$. a. Reaction in the Ratio 1:1. Synthesis of [2-Methyl-3*H*-indolium]1. 2-Methylindole (0.419 g, 3.13 mmol) was dissolved in 12 mL of CH_2Cl_2 and added at room temperature to a suspension of (C$_6$F$_5$)$_3$BOH$_2$ (1.66 g, 3.13 mmol) in 12 mL of pentane. The resulting light pink suspension was stirred for 6 days and constantly monitored via ^{1}H NMR, but the spectra did not change with time, showing that the reaction had occurred in a few minutes, affording stable products. The main component of the reaction mixture was [2-methyl-3*H*-indolium]**1**, together with a small amount (ca. 10%) of *N*-[B(C$_6$F$_5$)$_3$]-2-methyl-3*H*-indole,[5a] possibly due to the presence of some free B(C$_6$F$_5$)$_3$ in the starting (C$_6$F$_5$)$_3$BOH$_2$. ^{1}H NMR (CD_2Cl_2, 298 K): δ 2.66 (s, 3H, C*H*$_3$), 4.90 (br s, 4H, N*H*, O*H* and C*H*$_2$), 7.27−7.70 (m, 4H, Ar). ^{1}H NMR (CD_2Cl_2, 215 K): δ 2.42 (s, 1H, O*H*), 2.70 (s, 3H, CH$_3$), 4.17 (s, 2H, C*H*$_2$), 7.03 (m, 1H, N*H*), 7.28−7.54 (m, 3H, H5, H6, and H7), 7.57−7.71 (m, 1H, H4). COSY (CD_2Cl_2, 215 K): δ(^{1}H)/δ(^{1}H) 7.57−7.71/4.17 (H4/C*H*$_2$), 4.17/2.70 (C*H*$_2$/C*H*$_3$), 7.03/7.28−7.54 (N*H*/Ar). NOESY (CD_2Cl_2, 215 K): δ(^{1}H)/δ(^{1}H) 4.17/2.70 (C*H*$_2$/C*H*$_3$), 2.42/4.17 (O*H*/C*H*$_2$), 4.17/7.57−7.71 (C*H*$_2$/H4). Colorless crystals suitable for X-ray diffraction were obtained from a solution in CH_2Cl_2/pentane (9:1) stored at −20 °C for 5 days, which unexpectedly resulted to be the [2-methyl-3*H*-indolium]**3** salt.

b. Reaction in the ratio 1:2. Synthesis of [2-Methyl-3*H*-indolium]3. A solution of 2-methylindole (63.4 mg, 0.474 mmol, in 3 mL of CH_2Cl_2) was added at room temperature to a suspension of (C$_6$F$_5$)$_3$BOH$_2$ (507 mg, 0.957 mmol, in 5 mL of CH_2Cl_2) to give a pink suspension. A ^{1}H NMR analysis after 10 min of stirring showed the almost complete conversion to [2-methyl-3*H*-indolium]-**3**, together with traces of *N*-[B(C$_6$F$_5$)$_3$]-2-methyl-3*H*-indole.[5a] ^{1}H NMR (CD_2Cl_2, 298 K): δ 2.95 (s, 3H, C*H*$_3$), 4.49 (br s, 2H, C*H*$_2$), 6.86 (br s, 4H, N*H*, and O*H*'s), 7.53−7.79 (m, 4H, Ar).

Preparation of [NHEt$_3$]$^+$[(F$_5$C$_6$)$_3$BOB(C$_6$F$_5$)$_2$]$^-$ ([NHEt$_3$]4). A CD_2Cl_2 solution of (C$_6$F$_5$)$_2$BOH (413 mg, 1.14 mmol) was added at 0 °C to a suspension of B(C$_6$F$_5$)$_3$ (584 mg, 1.14 mmol) in CD_2Cl_2, the mixture was allowed to reach room temperature, and then 1 equiv of NEt$_3$ was added. Removal of the solvent at reduced pressure afforded a white solid characterized as the novel species [NHEt$_3$]**4** formed quantitatively. Colorless crystals suitable for X-ray analysis were obtained by cooling at −20 °C a solution of [NHEt$_3$]-**4** in a 2:1 mixture of pentane/dichloromethane. ^{1}H NMR (CD_2Cl_2, 298 K): δ 1.44 (t, 9H, C*H*$_3$, $^3J_{HH}$ = 7.2 Hz), 3.33 (q, 6H, C*H*$_2$, $^3J_{HH}$ = 7.4 Hz), 5.14 (br t, 1H, N*H*). ^{19}F NMR (CD_2Cl_2, 253 K): δ −134.11 (m, 4F$_{ortho}$), −134.68 (m, 6F$_{ortho}$), −154.37 (m, 2F$_{para}$), −161.55 (m, 3F$_{para}$), −163.49 (m, 4F$_{meta}$), −166.64 (m, 6F$_{meta}$).

X-ray Diffraction Structural Analysis. Crystal data for [C$_9$H$_{10}$N]-**3**: C$_{45}$H$_{13}$B$_2$F$_{30}$NO$_2$, M_r = 1191.18, triclinic, space group $P\bar{1}$ (No. 2), a = 12.606(4) Å, b = 12.910(4) Å, c = 14.040(4) Å, α = 85.99(1)°, β = 85.17(1)°, γ = 74.96(1)°, V = 2196.1(12) Å^3, Z = 2, T = 295(2) K, graphite-monochromated Mo Kα radiation (λ = 0.71073 Å), ρ_{calcd} = 1.801 g cm^{-3}, F(000) = 1172, colorless crystal, 0.44 × 0.26 mm × 0.26 mm^3, μ(Mo Kα) = 0.197 mm^{-1}, empirical absorption correction (SADABS,[44] 16298 symmetry-equivalent reflections, effective data-to-parameters ratio 9.1), minimum/maximum transmission factors 0.930/0.950, Bruker SMART diffractometer, ω scans ($\Delta\omega$ = 0.3°), 2400 frames each at 30 s of exposure, keeping the detector at 5.0 cm from the sample, 1.5° ≤ θ ≤ 29.0°, index ranges h = −17 → +17, k = −17 → +17, l = −19 → +19, 37730 reflections, 11650 of which are unique (R_{int} = 0.0290, R_σ = 0.0176), 7907 reflections with $I > 2\sigma(I)$, intensity decay 7%, solution by direct methods (SIR97[45]) and subsequent Fourier synthesis, anisotropic full-matrix least-squares refinement on F^2 using all reflections (SHELX97[46]), hydrogen atoms of hydroxo and aqua ligands evidenced in a difference Fourier map and refined isotropically without imposing any constraints, all other hydrogen atoms placed in idealized positions, data/parameters 11650/741, $S(F^2)$ = 1.076, $R[F, I > 2\sigma(I)]$ = 0.0456, $R_w(F^2$, all data) = 0.1461, weighting scheme $w = 1/[\sigma^2(F_o^2) + (0.085P)^2]$, where $P = (F_o^2 + 2F_c^2)/3$, maximum/minimum residual electron density 0.333/−0.278 e Å^{-3}.

Crystal data for [NHEt$_3$]**4**: C$_{36}$H$_{16}$B$_2$F$_{25}$NO, M_r = 975.12, monoclinic, space group $P2_1/c$ (No. 14), a = 14.411(4) Å, b = 11.741(3) Å, c = 22.080(7) Å, β = 104.44(1)°, V = 3617.9(18) Å^3, Z = 4, T = 90(2) K, graphite-monochromated Mo Kα radiation (λ = 0.71073 Å), ρ_{calcd} = 1.790 g cm^{-3}, F(000) = 1928, colorless crystal, 0.24 × 0.22 mm × 0.14 mm^3, μ(Mo Kα) = 0.196 mm^{-1}, empirical absorption correction (SADABS,[44] 30754 symmetry-equivalent reflections, effective data-to-parameters ratio 10.2), minimum/maximum transmission factors 0.945/0.973, Bruker SMART diffractometer, ω scans ($\Delta\omega$ = 0.3°), 2400 frames each at 20 s of exposure, keeping the detector at 5.0 cm from the sample, 1.5° ≤ θ ≤ 25.0°, index ranges h = −16 → +16, k = −13 → +13, l = −26 → +26, 41262 reflections, 6359 of which are unique (R_{int} = 0.0239, R_σ = 0.0149), 5836 reflections with $I > 2\sigma(I)$, no intensity decay, solution by direct methods (SIR97[45]) and subsequent Fourier synthesis, anisotropic full-matrix least-squares refinement on F^2 using all reflections (SHELX97[46]), hydrogen atoms placed in idealized positions, data/parameters 6359/596, $S(F^2)$ = 1.036, $R[F, I > 2\sigma(I)]$ = 0.0315, $R_w(F^2$, all data) = 0.0873, weighting scheme $w = 1/[\sigma^2(F_o^2) + (0.08P)^2 + 2P]$, where $P = (F_o^2 + 2F_c^2)/3$, maximum/minimum residual electron density 0.396/−0.213 e Å^{-3}.

Acknowledgment. T.B. and G.D. thank Basell Polyolefins for partial funding of this work. Thanks are also due to the Italian CNR (ISTM) for providing facilities for inert atmosphere and low-temperature experiments.

Supporting Information Available: Seven figures showing details of the NMR experiments. This material is available free of charge via the Internet at http://pubs.acs.org. CCDC 251191 and 251192 contain the supplementary crystallographic data for this paper. These data can be obtained free of charge via http://www.ccdc.cam.ac.uk/conts/retrieving.html (or from the CCDC, 12 Union Rd., Cambridge CB2 1EZ, U.K., fax +44-1223-336033, e-mail deposit@ccdc.cam.ac.uk).

IC0502168

(44) Sheldrick, G. M. *SADABS*; Universität Göttingen, Göttingen, Germany, 1996.
(45) Altomare, A.; Burla, M. C.; Camalli, M.; Cascarano, G. L.; Giacovazzo, C.; Guagliardi, A.; Moliterni, A. G. G.; Polidori, G.; Spagna, R. *J. Appl. Crystallogr.* **1999**, *32*, 115.
(46) Sheldrick, G. M. *SHELX97*; Universität Göttingen, Göttingen, Germany, 1997.